BMC Musculoskeletal Disorders

RESEARCH

Open Access

Clinical study of 3D printing template in the treatment of pediatric distal tibial epiphyseal fracture

Taotao Hui[1†], Jun Wang[1†], Yinghao Yu[1], Li Qiang[1], Haojuan Dong[1*] and Weifeng Lin[1*]

Abstract

Objective To investigate the clinical efficacy and safety of 3D printing template in the fixation of distal tibial epiphyseal fractures in children.

Methods A retrospective analysis was conducted on 57 cases of distal tibial epiphyseal fracture admitted to our hospital between January 2017 and January 2023. 27 patients underwent the conventional operative technique (conventional group), while the remaining 30 patients underwent the 3D printing template (3D printing template group). Exclusions comprised patients presenting with pathological fracture, neuromuscular disorder, metabolic disease, prior tibial fracture or instrumentation, and polytrauma. Additionally, individuals with a follow-up duration of less than 12 months or incomplete medical records were excluded. The reduction effect was evaluated using radiographs, and the times of fluoroscopy, operation time, time to union, and complications (such as infection or loss of reduction) were documented. Ankle joint function was assessed by the AOFAS score.

Results A total of 57 patients were divided into two groups: the conventional group, comprising 27 patients (14 males, 13 females), and the 3D printing template group, consisting of 30 patients (19 males, 11 females). Patients in both groups were followed up for at least one year, with an average of 2.3 years (1–3 years). The two groups exhibited no statistically significant differences in terms of sex, age, body weight, mechanism of injury, time from injury to surgery, Salter-Harris classification, or concomitant injuries. There was no significant difference in length of hospital stay, time to union, and limb length discrepancy between the two groups ($P > 0.05$). However, there was significantly less operative time in the 3D template group compared with the conventional group ($P < 0.05$). Higher intraoperative fluoroscopy frequency was observed in the conventional group than in the 3D template group ($P < 0.001$). However, the hospitalization expenses were higher in the 3D template group (3784 ± 315.7 $) than in the conventional group (3449 ± 550.6 $). No infection, nonunion, delayed union, malunion, loss of reduction, or premature epiphyseal closure between the two groups. Tendon adhesions were observed in 10 cases in the conventional group, contrasting with 12 cases in the 3D template group. In the final follow-up, AOFAS scores reflected excellence in 26 cases and goodness

†Taotao Hui and Jun Wang contributed equally to this work.

*Correspondence:
Haojuan Dong
huitt2335@163.com
Weifeng Lin
15150023018@163.com

Full list of author information is available at the end of the article

© The Author(s) 2025. **Open Access** This article is licensed under a Creative Commons Attribution-NonCommercial-NoDerivatives 4.0 International License, which permits any non-commercial use, sharing, distribution and reproduction in any medium or format, as long as you give appropriate credit to the original author(s) and the source, provide a link to the Creative Commons licence, and indicate if you modified the licensed material. You do not have permission under this licence to share adapted material derived from this article or parts of it. The images or other third party material in this article are included in the article's Creative Commons licence, unless indicated otherwise in a credit line to the material. If material is not included in the article's Creative Commons licence and your intended use is not permitted by statutory regulation or exceeds the permitted use, you will need to obtain permission directly from the copyright holder. To view a copy of this licence, visit http://creativecommons.org/licenses/by-nc-nd/4.0/.

in one in the conventional group, while excellence was noted in 28 cases and goodness in two in the 3D template group, culminating in an outstanding rate of 100% for both excellence and goodness.

Conclusion The conventional technique and 3D printing template technique both met the treatment requirements of distal tibial epiphyseal fractures. 3D printing guide plate provides a new method for distal tibial epiphyseal fractures with high accuracy and safety compared with traditional method by reducing the times of fluoroscopy and operating time.

Clinical trial number Not applicable.

Keywords 3D printing technology, Template, Distal tibial epihyseal fracture, Position, Cost-effectiveness

Introduction

Distal tibial epiphyseal fractures are common injuries in the pediatric population [1–3]. If not properly addressed with active anatomical reduction, this can lead to traumatic arthritis, premature epiphyseal closure, ankle deformity, and other complications. The type of injury, its severity, and the treatment all have a direct effect on the function and shape of the ankle joint [4]. Salter-Harris classification is the most commonly used anatomic system used to categorize fractures that occur in the growth plate of pediatric patients [5]. It is simple, and each injury type has prognostic significance.

For cases involving salter-Harris type I/II distal tibial epiphyseal fractures, conservative treatment is recommended and close monitoring of patients is essential. If salter-Harris type II fractures of the distal tibia exhibit displacement equal to or greater than 3 mm, closed reduction with casting is the preferred treatment. In cases where closed reduction is unsuccessful, open reduction becomes necessary [6]. Surgery should be considered for individuals with Salter-Harris type III/IV distal tibial epiphyseal fractures to achieve an anatomically precise reduction and secure rigid internal fixation, thus decreasing the likelihood of premature epiphyseal closure. Lag screw fixation is advantageous in that it results in a lower rate of premature epiphyseal closure, whereas Kirschner wire fixation offers the advantage of reducing the need for additional anesthesia and surgery [7]. Despite the treatment method selected, it remains challenging to accurately place the screw, cause minimal trauma, and limit the operation time and fluoroscopy exposure. The utilization of 3D printing technology, a relatively recent advancement, is progressively growing within the field of orthopedics for the production of customized guide plates for diverse surgical procedures [8–12].

The objective of this study was to assess the comparative efficacy and safety of screw placement as well as functional outcomes among pediatric patients with distal tibial epiphyseal fractures undergoing either conventional technique or utilizing a 3D printing template.

Patients and methods

Exclusion criteria and inclusion criteria

Inclusion criteria was as follows: those under 16 years of age at the time of injury and fracture confirmed by a radiograph, history of trauma, acute fracture, Salter-Harris II and IV (triplane) fractures. Patients aged sixteen and above at the time of the surgery, those with open fractures, pathologic fractures, polytrauma, preoperative radiographs showing distal tibial epiphyseal closure, and neurological, metabolic, or endocrine disorders were excluded from the criteria. Additionally, individuals with a follow-up duration of less than 12 months or incomplete medical records were excluded.

From January 2017 to January 2023, 57 consecutive patients, including 33 males and 24 females were retrospectively reviewed. The patients were divided into two groups, (1) conventional operative technique (conventional group) and (2) 3D printing template (3D printing template group), as per the surgery they underwent. Out of 57 patients, 27 patients were included in the conventional group, and the remaining 30 patients were included in the 3D printing template group. Preoperative data were retrieved from the hospital database, while postoperative data were obtained during follow-up visits. To mitigate potential bias, all clinical evaluations were conducted by a Ph.D. scholar uninvolved in the surgical procedures.

This study was approved by the Ethical Committee of our hospital. All methods adhered to pertinent guidelines and regulations. Written informed consent was obtained from the legal guardians of the patients subsequent to thorough explanation of the study's purpose and procedures.

Preoperative planning and simulation

In lateral X-rays of the ankle, the coronal fracture line of the tibial metaphysis is often obscured by the fibula. Due to its high resolution, CT can detect fracture lines that are difficult to identify on conventional X-rays. Moreover, CT provides a clear visualization of the fracture line's orientation in cross-sectional images, which is crucial for preoperative planning and predicting the direction of nail

insertion. Therefore, both groups underwent preoperative CT examinations.

The 3D template was generated as follows: CT DICOM data were imported into FirePlus3D V1.0 software (Shanghai Black Flame Medical Company, China) for fracture segmentation and virtual reduction. A patient-specific guide plate (1.0 mm thickness) was designed to match the distal tibial anatomy, with puncture trajectories preplanned to avoid the physis. The model was printed using photosensitive resin and sterilized with ethylene oxide prior to surgery (It only took 1 day for the whole process, including the design, printing and sterilization).

Surgical technique

The surgical procedures were carried out by the same surgeon.

Under general anesthesia, the patient was positioned on the operating table. After the lower limb was disinfected and draped, the tourniquet was secured. A straight incision about 5 cm long was made on the anterolateral surface of the medial malleolus. The soft tissue was incised to expose the fracture fragment. All soft tissue in this area was cleared, but the periosteum was preserved as much as possible. The fragment of the fracture was gently exposed and the soft tissue embedded in the fragment was removed, especially the periosteum. The front of the ankle joint was exposed and the fracture was anatomically reduced after continuous traction. Fluoroscopy confirmed the fracture was well-reduced.

3D printing template group: 3D printing guide plate was attached to the surface of the distal tibial according to the reference. 1.0–1.2 mm Kirschner wires were inserted into the hole in the guide plate to fix the segment. Fluoroscopy verification revealed that the fracture had been properly reduced and the Kirschner wires were in the correct position. If the reduction was anatomically accurate, Kirschner wires were replaced with the lag screws (3.5–4.0 mm) (Fig. 1). A Diagram is shown in Figs. 2 and 3.

Conventional group: The fracture was reduced under direct visualization with confirmation of radiographic reduction with c-arm image intensification intraoperatively. Initially, the fractured end was immobilized into a

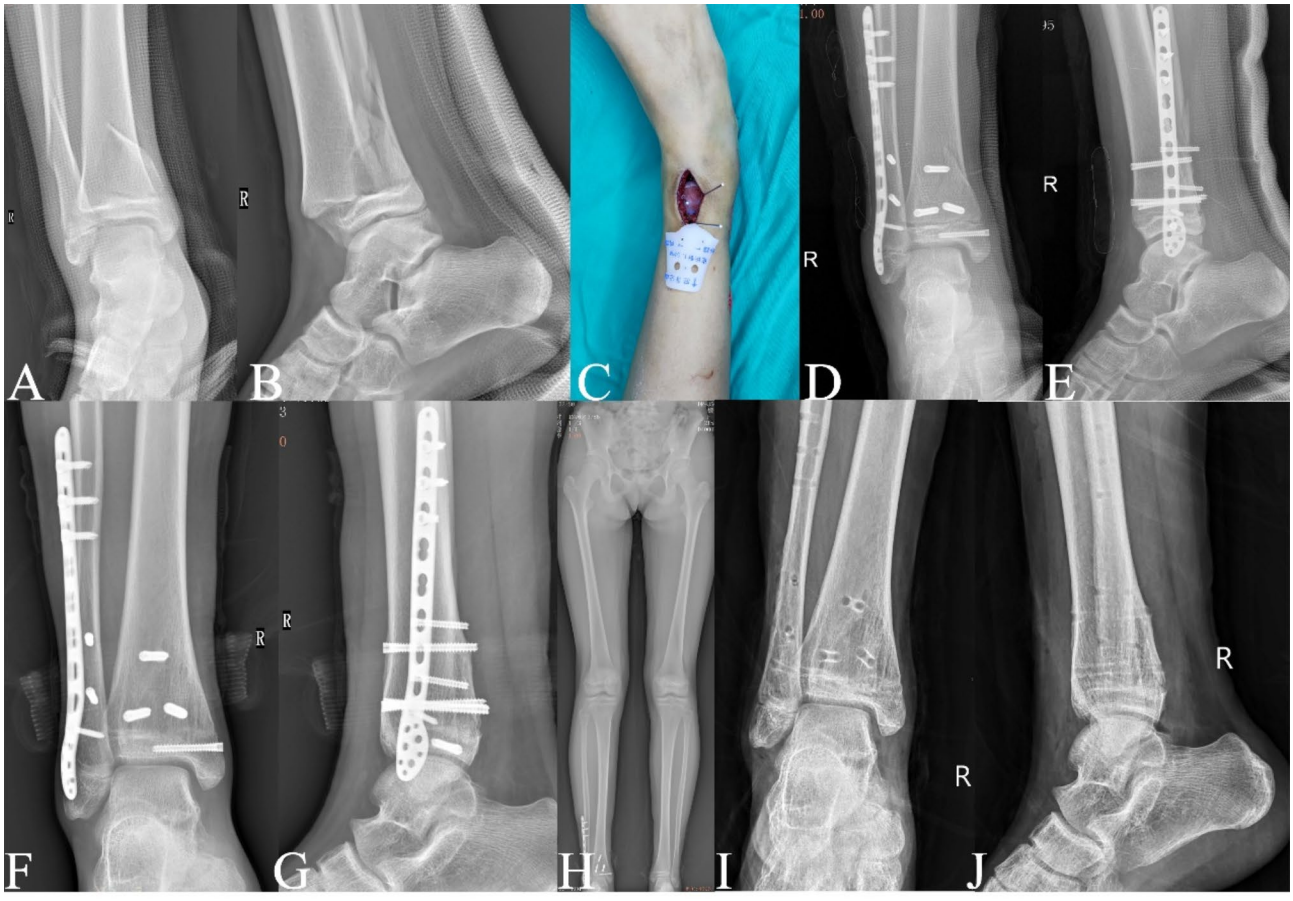

Fig. 1 Case example: a girl, fell from her bike. **A** and **B**, Anteroposterior and lateral radiographs demonstrating a tibial epiphyseal fracture on the right side (Salter–Harris IV). **C**, Construction and application of a 3D printing template intraoperatively. **D** and **E**, Radiographs taken postoperatively. **F**, **G** and **H**, Radiographs taken after 12 months of follow-up. **I** and **J**, Radiographs taken after removal of hardware

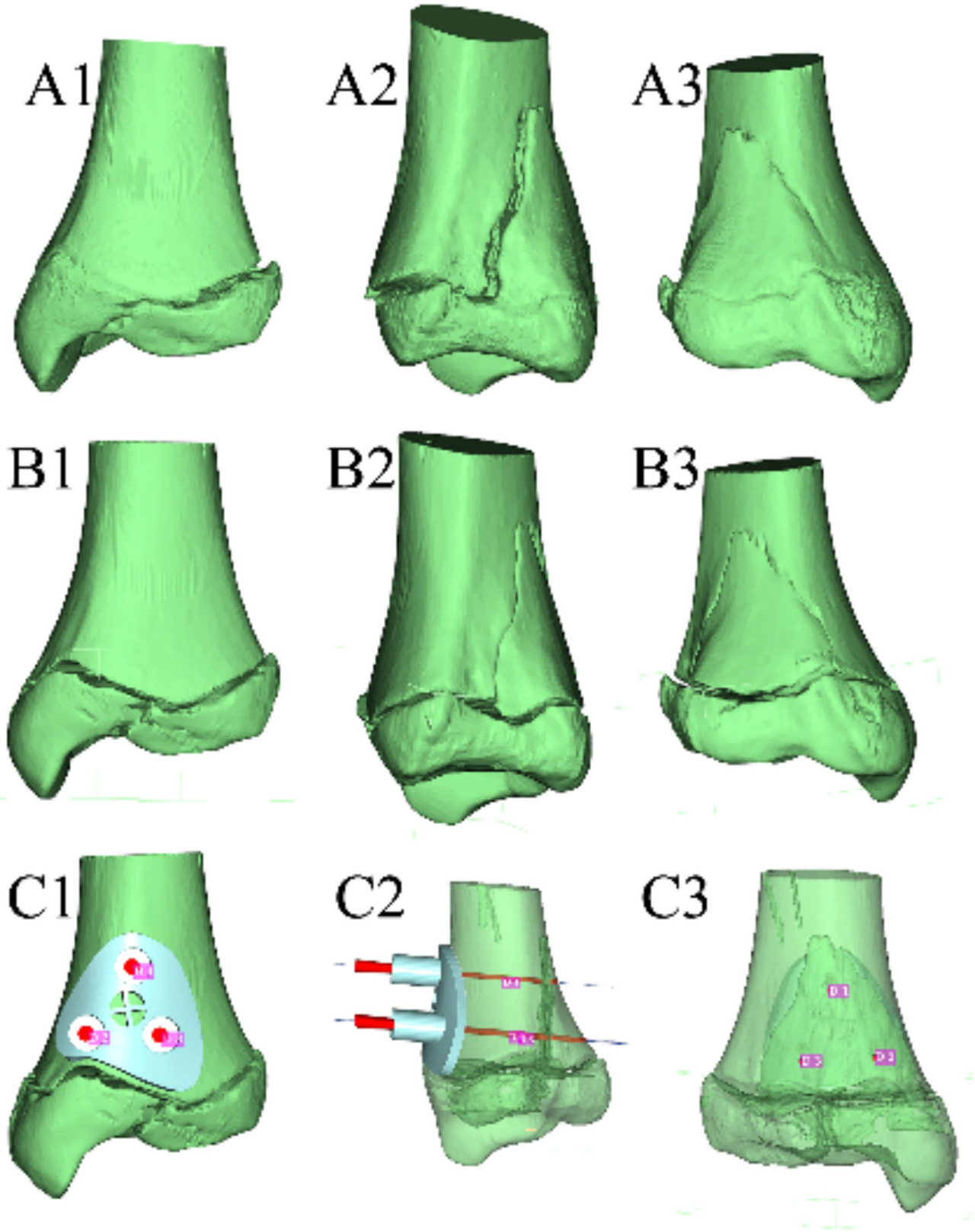

Fig. 2 Puncture simulation with 3D printing template and the process of fixation of Salter-Harris Type IV fracture. Anterior **(A1)**, lateral **(A2)** and posterior view **(A3)** without reduction. Anterior **(B1)**, lateral **(B2)** and posterior view **(B3)** after reduction. Equilateral triangle fixation of anterior **(C1)**, lateral **(C2)** and posterior view **(C3)** with 3D printing template

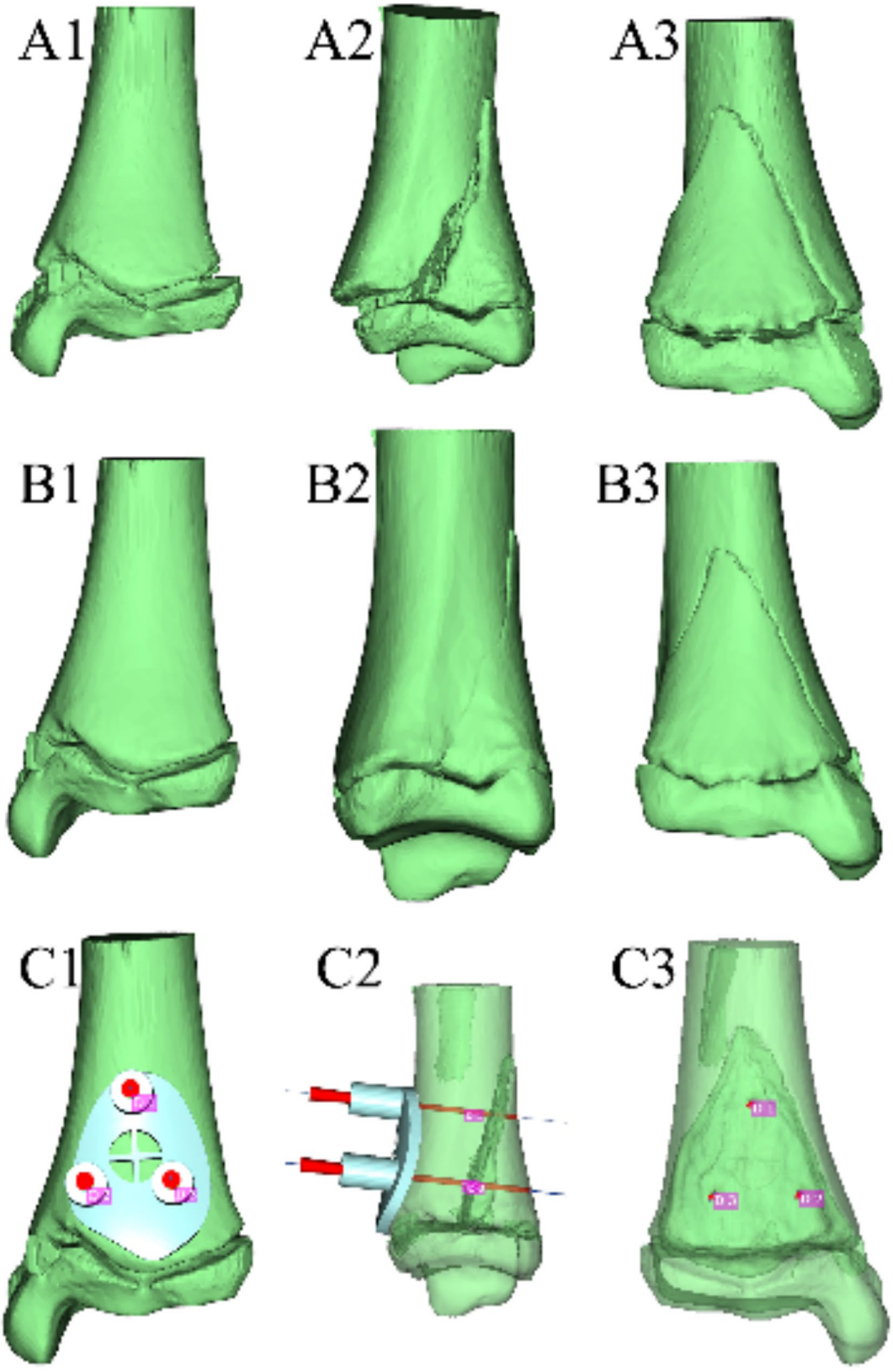

Fig. 3 Puncture simulation with 3D printing template and the process of fixation of Salter-Harris Type II fracture. Anterior **(A1)**, lateral **(A2)** and posterior view **(A3)** without reduction. Anterior **(B1)**, lateral **(B2)** and posterior view **(B3)** after reduction. Equilateral triangle fixation of anterior **(C1)**, lateral **(C2)** and posterior view **(C3)** with 3D printing template

Table 1 Parameters of patients in the conventional and the 3D template group

Variables	Conventional (*n* = 27)	3D Template (*n* = 30)	*p*-value
Age (year)	12.1±1.8	12.4±1.5	0.414
Sex			
Female	13	11	0.381
Male	14	19	
BMI (Kg/m^2)	20.8±2.9	22.6±4.3	0.088
Time from injury to surgery	4.2±1.3	3.8±1.1	0.191
Mechanism of injury			
Falling	20	26	0.229
Sprain	7	4	
Salter-Harris classification			
II	11	12	0.955
IV	16	18	

*p value < 0.05

BMI = Body mass index

finalized configuration utilizing 3 vertical fracture lines of Kirschner wires (1.0–1.2 mm). Fluoroscopy verification confirmed the proper reduction of the fracture and the correct positioning of the Kirschner wires. In cases where the reduction was anatomically precise, Kirschner wires were exchanged for lag screws (3.5–4.0 mm).

Observation parameters

The evaluation index was selected as the times of fluoroscopy, operation time, time to union, hospitalization time, hospitalization expenses, limb length discrepancy, premature epiphyseal closure rate by X-ray at the last follow-up and complications. The AOFAS ankle function score was recorded at the last follow-up.

Statistical analysis

We did a power analysis to justify the sample size through PASS software, as this is vital to assess the study's potential for reliable findings and avoid Type II errors. All statistical analysis was performed using an α of 0.05. Statistical analysis was performed using SPSS software (version 23.0; SPSS Inc., Chicago, Illinois, USA). Categorical data were evaluated employing the Chi-square ($\chi 2$) test, whereas continuous data underwent analysis via Student's t-test. In instances involving smaller subject groups of interest, the Fisher exact test was utilized. Data were presented as mean ± SD (range), median (range), or n (%).

Postoperative care

A short-leg plaster cast was used to immobilize the ankle in a neutral position for 6–8 weeks. It is advised to elevate the injured limb. X-ray examination is conducted to evaluate the healing process of the fracture. if the healing is successful, walking with crutches and weight-bearing exercises may commence. The screws can be extracted 6–12 months post-surgery.

Table 2 Clinical parameters of the conventional and the 3D template group

Variables	Conventional (*n* = 27)	3D Template (*n* = 30)	*p*-value
Operating time (min)	80.1 ± 45.4	62.1 ± 21.8	< 0.05
Length of stay (day)	10.5 ± 4.4	9.5 ± 6.0	0.448
Hospitalization expenses ($)	3449 ± 550.6	3784 ± 315.7	< 0.05
Fluoroscopy (times)	10.7 ± 2.2	6.4 ± 1.3	< 0.001
Time to union (week)	9.6 ± 4.4	9.6 ± 5.7	0.999
Limb length discrepancy (cm)	0.1±0.2	0.1±0.2	0.980

*p value < 0.05

2 Results

As shown in Tables 1 and 27 patients, including 14 males and 13 females, were included in the conventional group, whereas 30 patients, including 19 males and 11 females, were included in the 3D printing template group ($P = 0.381$). The average age of patients in the conventional group was 12.1 ± 1.8 years, and that of 3D printing template group was 12.4 ± 1.5 years ($P = 0.414$). Patients in both groups were followed up for at least one year, with an average of 2.3 years (1–3 years). There was no significant difference between the two groups concerning sex, age, body mass index, duration from injury to surgery, injury mechanism, and Salter-Harris classification.

As shown in Table 2, the times of fluoroscopy significantly differed between the conventional group (10.7 ± 2.2 times) and the 3D printing template group (6.4 ± 1.3 times) ($P < 0.001$). The mean duration of the operative procedure was faster in the 3D printing template group (62.1 ± 21.8 min) than those in the conventional group (80.1 ± 45.4 min) ($P < 0.05$). A difference ($P < 0.05$) in hospitalization costs was observed between the conventional group (3449 ± 550.6 $) and the 3D printing template group (3784 ± 315.7 $). There was no significant difference in length of hospital stay, time to union, and limb length discrepancy between the two groups ($P > 0.05$). The higher hospitalization costs in the 3D printing group were attributed to expenses associated with 3D model printing materials (photosensitive resin), and specialized software licensing.

As shown in Table 3, no infection, nonunion, delayed union, malunion, loss of reduction, or premature epiphyseal closure were observed between the two groups. Tendon adhesions were observed in 10 cases in the conventional group, contrasting with 12 cases in the 3D template group.

According to the AOFAS ankle function score, no significant differences were found between the two groups. All patients had excellent or good outcomes in the both groups. The mean AOFAS score improvement in both

Table 3 Complications after surgery

Complication	Conventional ($n=27$)	3D Template ($n=30$)	p-value
Loss of reduction	0	0	> 0.999
Non-union	0	0	> 0.999
Delayed union	0	0	> 0.999
Malunion	0	0	> 0.999
Infection	0	0	> 0.999
Adhesion of tendon	10	12	0.819
Premature epiphyseal closure	0	0	> 0.999

*p value < 0.05

groups exceeded the established minimal clinically important difference (MCID) threshold of 10 points for ankle fractures, indicating clinically meaningful outcomes [13].

Discussion

Following distal radius epiphyseal injury, distal tibial epiphyseal injury is the second most common injury [14]. Treatment options for distal tibial epiphyseal fractures include both surgical and non-surgical approaches [15]. The surgical procedure involved both closed and open reduction, with internal fixation being either percutaneous Kirschner wire or lag screws [16]. Jie Wen et al. determined that both lag screw and Kirschner wire fixation techniques can achieve successful clinical outcomes for triplane distal tibial epiphyseal fracture. While lag screw fixation has a lower rate of premature epiphyseal closure, Kirschner wire fixation has the advantage of requiring only one anesthesia and surgery. If closed reduction does not result in the maintenance of the fracture fragment or if a satisfactory result of less than 2 mm is still not achieved, open reduction should be considered to determine if there is any soft tissue or periosteum entrapment preventing reduction [17]. As suggested by Schnetzler et al. [18], the reduction of distal tibial epiphyseal fractures should be kept to a minimum of 2 mm, as the fracture gap larger than 3 mm puts the individual at a greater risk of closure before the expected time.

The key to the successful fixation of fracture fragments is the establishment of a secure position; for this purpose, 3D printing guide plates have been designed to enhance the accuracy and safety of puncture positioning. By contrast, the traditional method relies on the physician's experience and multiple X-rays, but these can cause radiation damage to the patient and the surgeon, and require the surgeon to have a high level of skill and a lengthy period of training. Use of CT scan with or without 3D reconstruction is beneficial in understanding the fracture anatomy and improving the accuracy of screw placement for displaced distal tibial fractures previously [19–25].

A 3D guide plate was developed and applied in this study to enhance the accuracy of screw placement and guide the direction and angle of the positioning needle during puncture for optimal stability. This improved the accuracy of fracture fragments and simplified the process of positioning. Furthermore, the 3D reconstruction model theoretically gave patients and their families a more accurate grasp of the surgical techniques and potential risks, which is beneficial for the planning of clinical and surgical plans, thus enhancing patients' faith in doctors and creating a more harmonious doctor-patient relationship [26]. In our study, the times of intraoperative fluoroscopy in the 3D printing group was significantly less than those in the conventional group, which directly shortened the operation time. However, the implementation of 3D printing technology involved material and the use of 3D printing required trained personnel, increasing labor costs, the patients in the 3D printing template group had higher hospitalization costs.

This research project employed 3D printing to create a personalized guide plate. The growth plate was chosen as a bone marker, and the puncture guide plate was reconstructed based on the CT DICOM data, which was imported into FirePlus3D V1.0 software (Shanghai Black flame medical company in China) to simulate the fracture. The base of the guide plate was designed to be approximately 1 mm thick. Taking into account the three-dimensional reconstruction of the fracture fragment, the angle, and depth of the puncture hole of the guide plate were determined with a substantial safety gap, and the internal diameter of the puncture hole was designed to be 1.2 mm following the type of the puncture needle. The enlarged internal diameter of the puncture hole would result in an increased instability of the puncture needle, potentially resulting in an alteration of the puncture angle. The number and distribution of screws are primarily determined by the size of the fracture fragment. The screws should be arranged in an equilateral triangle to maximize stress distribution. However, this arrangement needs to be verified through biomechanical studies in the future.

All patients underwent X-ray verification during the operation, with successful needle puncture achieved in every case (100.00%) using a guide plate. The preoperative design was followed in terms of entry point, depth, and puncture angle, enabling a shorter puncture time and reduced intraoperative bleeding. Upon the last follow-up visit, all patients in this study had successful results from the surgical treatment of distal tibial epiphyseal fractures, with no restrictions to ankle joint mobility, and the AOFAS scores were excellent. The Salter-Harris classification does not affect the results of pediatric distal tibial epiphyseal fractures. Compare with the Salter-Harris Type II fractures, Salter-Harris Type IV fractures often require more operating time, higher hospitalization expenses, more times of fluoroscopy and higher

complication rates, however, there is no statistically significant difference in terms of Salter-Harris classification between two groups. Tendon adhesions were attributed to perioperative soft tissue handling rather than implant position. All cases resolved with physiotherapy; no revision surgeries were required. Implants (3.5–4.0 mm lag screws) were electively removed at 6–12 months post-op, with no growth disturbances observed at final follow-up. In our study, although tendon adhesions were observed in both groups, the extensor hallucis longus showed mild adhesions. Tendinolysis was frequently performed concurrently with hardware removal.

In sum, the research conducted to investigate the utilization of 3D printing plates in the stabilization of pediatric distal tibial epiphyseal fractures has yielded promising outcomes in terms of efficacy and safety. The 3D printing guide plates can increase the accuracy of lag screw placement and reduce fluoroscopy and operating time, which render it an attractive choice for pediatric orthopedics.

To further validate these findings, however, it is imperative to conduct additional studies to assess long-term consequences, perfect the design and materials, and create standardized procedures for its utilization. Comparative studies evaluating the biomechanical characteristics of 3D printing plates versus traditional surgical techniques can provide valuable information in this regard.

The study was limited by its short duration, and further clinical results with longer follow-ups are necessary. Further investigation is necessary to assess the long-term effects of 3D printing guide plates used in the fixation of pediatric distal tibial epiphyseal fractures. Longitudinal studies can offer insight into the stability of the fixation, any potential issues such as malunion or growth issues, and the patient's functional outcomes. While this retrospective study provides preliminary evidence for 3D printing applications in pediatric fractures, we acknowledge that the sample size ($n = 57$) may limit generalizability. Future prospective randomized trials with larger cohorts are warranted to validate these findings. Such studies could further assess long-term growth outcomes and cost-effectiveness.

Conclusion

3D printing guide plate provides a new method for distal tibial epiphyseal fractures with high accuracy and safety compared with traditional method by reducing the times of fluoroscopy and operating time. Hence, further investigation in a clinical setting is warranted. However, compared to conventional treatments, the use of 3D printing may entail higher costs for patients.

Author contributions

Taotao Hui, MD (Contribution: performed measurements, manuscript preparation)Jun Wang, MD (Contribution: study design, performed measurements, manuscript preparation)Yinghao Yu, MD (Contribution: data analysis)Li Qiang, BS (Contribution: data analysis)Haojuan Dong, BS (Contribution: provision of study materials or patients)Weifeng, Lin, BS (Contribution: conception and design).

Funding

This study was provided by Binhu Medical Expert Team of "Light of Binhu Program".

Data availability

The datasets generated and analyzed during the current study are available from the corresponding author on reasonable request.

Declarations

Ethics approval and consent to participation

The study protocol was approved by the Human Ethics Research Board of Wuxi No.9 People's Hospital Affiliated to Soochow University. All procedures and methods were carried out in accordance with a Declaration of Helsinki regulation and guidelines. All patient's legal guardians provided informed consent for participation in the study.

Consent for publication

Not application.

Conflict of interest

The authors declare that they have no known competing financial interests or personal relationships that could have appeared to influence the work reported in this paper.

Author details

[1]Department of Pediatric Orthopedics, Wuxi No.9 People's Hospital Affiliated to Soochow University, Liangxi Road, Wuxi 214000, Jiangsu Province, China

Received: 8 January 2025 / Accepted: 8 April 2025
Published online: 15 April 2025

References

1. Michael T, Rohmiller M, Tracey P, Gaynor MA, Jeff Pawelek BS, Mubarak SJ. MD: Salter-Harris I and II fractures of the distal tibia: does mechanism of injury relate to premature physeal closure? 2006, May-Jun;26(3):322-8.
2. Spiegel PG, Cooperman DR, Laros GS. J Bone Joint Surg Am. 1978;60(8):1046–50.
3. Wuerz TH, Gurd DP. Pediatric physeal ankle fracture. J Am Acad Orthop Surg. 2013;21(4):234–44.
4. Kärrholm J, Hansson LI, Svensson K. Prediction of growth pattern after ankle fractures in children. J Pediatr Orthop. 1983;3(3):319–25.
5. Salter RBHW. Injuries involving the epiphyseal plate. J Bone Joint Surg Am. 1963;45:587–622.
6. Thomas RA, Hennrikus WL. Treatment and outcomes of distal tibia Salter Harris II fractures. Injury. 2020;51(3):636–41.
7. Tang Z, Xiang F, Arthur VD, Xiao S, Wen J, Liu H, Li X, Fang K, Zeng M, Cao S, et al. Comparison of mid-term clinical results between lag screw fixation and Kirschner wire fixation after close reduction in adolescent triplane distal tibia epiphyseal fracture. Foot Ankle Surg. 2022;28(8):1440–3.
8. Meng M, Wang J, Huang H, Liu X, Zhang J, Li Z. 3D printing metal implants in orthopedic surgery: methods, applications and future prospects. J Orthop Translat. 2023;42:94–112.
9. Skelley NW, Smith MJ, Ma R, Cook JL. Three-dimensional printing technology in orthopaedics. J Am Acad Orthop Surg. 2019;27(24):918–25.
10. Mulford JS, Babazadeh S, Mackay N. Three-dimensional printing in orthopaedic surgery: review of current and future applications. ANZ J Surg. 2016;86(9):648–53.
11. Wixted CM, Peterson JR, Kadakia RJ, Adams SB. Three-dimensional printing in orthopaedic surgery: current applications and future developments. J Am Acad Orthop Surg Glob Res Rev. 2021;5(4):e20. 00230– 00211.
12. Jiang M, Chen G, Coles-Black J, Chuen J, Hardidge A. Three-dimensional printing in orthopaedic preoperative planning improves intraoperative metrics: a systematic review. ANZ J Surg. 2020;90(3):243–50.

13. SooHoo NF, Samimi DB, Vyas RM, Botzler T. Evaluation of the validity of the foot function index in measuring outcomes in patients with foot and ankle disorders. Foot Ankle Int. 2006;27(1):38–42.
14. Podeszwa DA, Mubarak SJ. Physeal fractures of the distal tibia and fibula (Salter-Harris type I, II, III, and IV fractures). J Pediatr Orthop. 2012;32(Suppl 1):S62–68.
15. Cai H, Wang Z, Cai H. Surgical indications for distal tibial epiphyseal fractures in children. Orthopedics. 2015;38(3):e189–195.
16. Ertl JP, Barrack RL, Alexander AH, VanBuecken K. Triplane fracture of the distal tibial epiphysis. Long-term follow-up. J Bone Joint Surg Am. 1988;70(7):967–76.
17. Rapariz JM, Ocete G, González-Herranz P, López-Mondejar JA, Domenech J, Burgos J, Amaya S. Distal tibial triplane fractures: long-term follow-up. J Pediatr Orthop. 1996;16(1):113–8.
18. Spiegel PG, Cooperman DR, Laros GS. Epiphyseal fractures of the distal ends of the tibia and fibula. A retrospective study of two hundred and thirty-seven cases in children. J Bone Joint Surg Am. 1978;60(8):1046–50.
19. Dinesh Thawrani M, Victoria Kuester MD, Peter G, Gabos MD, Richard W, Kruse MBA, Aaron DO, Littleton G, BSc KJ, Rogers, PhD ATC. Laurens Holmes, PhD, and Mihir M. Thacker, MD: Reliability and Necessity of Computerized Tomography in Distal Tibial Physeal Injuries. *J Pediatr Orthop* 2011, Oct-Nov;31(7):745– 50.
20. Cutler L, Dhukuram AMV, Bass A. Do CT scans aid assessment of distal tibial physeal fractures? J Bone Joint Surg Br. Mar; 2004;86(2):239–43.
21. Xiong L, Li X, Li H, Chen Z, Xiao T. The efficacy of 3D printing-assisted surgery for traumatic fracture: a meta-analysis. Postgrad Med J. 2019;95(1126):414–9.
22. Neijhoft J, Henrich D, Mors K, Marzi I, Janko M. Visualization of complicated fractures by 3D-printed models for teaching and surgery: hands-on transitional fractures of the ankle. Eur J Trauma Emerg Surg. 2022;48(5):3923–31.
23. Nenopoulos A, Beslikas T, Gigis I, Sayegh F, Christoforidis I, Hatzokos I. The role of CT in diagnosis and treatment of distal tibial fractures with intra-articular involvement in children. Injury. 2015;46(11):2177–80.
24. Jones S, Phillips N, Ali F, Fernandes JA, Flowers MJ, Smith TW. Triplane fractures of the distal tibia requiring open reduction and internal fixation. Preoperative planning using computed tomography. Injury. 2003;34(4):293–8.
25. Zhao J, Ma Y, Han D, Jin Y. [Application of three-dimensional printing in the operation of distal tibia fracture involving epiphyseal plate injury for teenagers]. Zhongguo Xiu Fu Chong Jian Wai Ke Za Zhi. 2017;31(10):1195–9.
26. Keyu G, Shuaishuai L, Raj A, Shuofeng L, Shuai L, Yuan Z, Haitao Z, Junqi W. A 3D printing personalized percutaneous puncture guide access plate for percutaneous nephrolithotomy: a pilot study. BMC Urol. 2021;21(1):184.

Publisher's note

Springer Nature remains neutral with regard to jurisdictional claims in published maps and institutional affiliations.